Chemical Senses, 2019, Vol 44, 583–591
doi:10.1093/chemse/bjz052
Original Article
Advance Access publication 17 August 2019

OXFORD

Original Article

Initial Characterization of a Subpopulation of Inherent Oscillatory Mammalian Olfactory Receptor Neurons

Kirill Ukhanov[1,4], Yuriy V. Bobkov[2,4], Jeffrey R. Martens[1,4] and Barry W. Ache[2,3,4,5]

[1]Department of Pharmacology and Therapeutics, University of Florida, Gainesville, FL 32610, USA, [2]Whitney Laboratory, University of Florida, [3]Departments of Biology and Neuroscience, University of Florida, [4]Center for Smell and Taste, University of Florida, Gainesville, FL 32610, USA and [5]McKnight Brain Institute, University of Florida, Gainesville, FL 32610, USA

Correspondence to be sent to: Barry W. Ache, Whitney Laboratory, Center for Smell and Taste, University of Florida, PO Box 100127, Fed Ex: 1149 Newell Dr., Gainesville, FL 32610, LG-101D. e-mail: bwa@whitney.ufl.edu

Editorial Decision 31 July 2019.

Abstract

Published evidence suggests that inherent rhythmically active or "bursting" primary olfactory receptor neurons (bORNs) in crustaceans have the previously undescribed functional property of encoding olfactory information by having their rhythmicity entrained by the odor stimulus. In order to determine whether such bORN-based encoding is a fundamental feature of olfaction that extends beyond crustaceans, we patch-clamped bORN-like ORNs in mice, characterized their dynamic properties, and show they align with the dynamic properties of lobster bORNs. We then characterized bORN-like activity by imaging the olfactory epithelium of OMP-GCaMP6f mice. Next, we showed rhythmic activity is not dependent upon the endogenous OR by patching ORNs in OR/GFP mice. Lastly, we showed the properties of bORN-like ORNs characterized in mice generalize to rats. Our findings suggest encoding odor time should be viewed as a fundamental feature of olfaction with the potential to be used to navigate odor plumes in animals as diverse as crustaceans and mammals.

Key words: mouse, olfactory coding, patch clamp, primary receptor cells, scene analysis

Introduction

There have been intermittent reports of oscillations in the olfactory periphery of diverse animals going back many years, some just mentioned in passing and some considered imposed. Particularly compelling were reports of oscillatory responses of olfactory receptor neurons (ORNs) in amphibians (Reisert and Matthews 2001a) and mice (Sicard 1986; Reisert and Matthews 2001b). We were intrigued by these findings when we found inherent oscillatory ORNs in the lobster olfactory organ, which we called "bursting" ORNs (bORNs) and were able to more fully characterize their dynamic characteristics and computationally model their potential functionality (Bobkov and Ache 2007; Park et al. 2014). We were especially intrigued by the earlier findings knowing that lobster bORNs have 3 previously undescribed functional properties. First, they encode olfactory information by having their rhythmicity entrained by the odor stimulus; they do not discharge phaso-tonically as do canonical ORNs. Second, as a population, they can accurately encode the interval since the last odor encounter up to tens of seconds using information inherent in the olfactory modality, that is, they can "smell time." Third and particularly interesting is that as a population they instantaneously encode the interval since the last odor encounter without the need to implicate memory.

Given the structure to the intermittency inherent in turbulent odor plumes (e.g., Shraiman et al. 2000; Vickers et al. 2001; Vergassola et al. 2007; Celani et al. 2014; Riffell et al. 2014), the ability of bORNs to encode the time between "whiffs" would provide a novel way to extract signal intermittency and help navigate turbulent plumes. Indeed, computational modeling showed that a simulated lobster "animat" can navigate simulated odor plumes with considerable more efficiency using odor time than odor concentration (Park et al. 2016). Finding the source of an odor is as fundamental to understanding olfaction as is identifying the nature of the odor itself, one with strong practical application. Thus, we were motivated to determine if bORN-based encoding is a fundamental feature of olfaction that extends beyond crustaceans. In particular, based on the earlier findings, we were motivated to determine the extent to which bORN-like ORNs also characterize the mammalian olfactory periphery.

In the present study, we recorded from bORN-like ORNs in mice and characterized their dynamic properties. We then characterized bORN-like activity by imaging the olfactory epithelium of OMP-GCaMP6f mice. Next, we compared their odor specificity to that of canonical ORNs by patching ORNs in OR/green fluorescent protein (GFP) mice. We showed the properties of bORN-like ORNs characterized in mice generalize to rats. Our findings suggest that encoding odor time is a fundamental feature of olfaction with the potential to be used to navigate odor plumes in animals as diverse as crustaceans and mammals.

Materials and Methods

Animals and semi-intact olfactory epithelium preparation

Adult Sprague-Dawley rats 4–6 weeks old (purchased from Charles River), wild-type (WT) C57/BI6 mice 2–3 months old (purchased from Harlan Labs), and several transgenic mouse strains 2–3 months old were used in the study. Mouse lines expressing GFP under the promotors for OR M71 and SR1 (M71/SR1-ires-tauGFP) and I7 (I7>M71-ires-tauGFP) were originally developed by Dr Peter Mombaerts (Max Planck Institute for Molecular Neurogenetics) and generously provided by Dr Minghong Ma (University of Pennsylvania). The M71/SR1 mouse was originally generated by crossing M71-ires-tauGFP (Bozza et al. 2002) and SR1-ires-tauGFP lines (Grosmaitre et al. 2009). An olfactory marker protein (OMP)-GCaMP6f mouse line was generated by crossing OMP-Cre mice (JAX Labs, stock #006668) with Rosa26^{loxP}-GCaMP6f mice (JAX Labs stock #028865). The Rosa26^{loxP}-GCaMP6f mouse line was generated (Madisen et al., Neuron 2015). Only animals heterozygous for OMP/Cre were used in the experiments, assuming one allele of OMP would maintain the wild-type phenotype of ORNs. The correct genotype was confirmed by PCR for each mouse strain. All animal handling, breeding, and experimental procedures were carried out according to the University of Florida Institutional Animal Care and Use Committee (IACUC) animal protocols. Animals of both sexes were used in these experiments.

Animals were euthanized using gaseous carbon dioxide according to the protocol approved by the University of Florida IACUC. The turbinates and septum were dissected and kept on ice in a Petri dish filled with freshly oxygenated ice-cold modified artificial cerebrospinal fluid (ACSF) saturated with 95% O2 and 5% CO2, containing (mM): 120 NaCl, 25 NaHCO3, 3 KCl, 1.25 Na2HPO4, 1 MgSO4, 1.8 CaCl2, and 15 glucose.

Electrophysiological recording from ORNs

Extracellular action potentials were recorded in situ from the dendritic knobs of ORNs in a piece of the main olfactory epithelium (MOE) in oxygenated ACSF using patch-clamp recording in the loose-patch configuration (e.g., Connelly et al. 2013). The dendritic knobs were visualized using Nomarski contrast on an upright microscope (Zeiss Axioskop 2FS, Carl Zeiss Microimaging) equipped with a 40x/NA0.75 water-immersion objective and a cooled CCD camera (ORCA2, Hamamatsu) under control of the imaging software HCImage (Hamamatsu). To identify dendritic knobs of the GFP-tagged ORNs, the tissue was illuminated using a standard enhanced green fluorescent protein (EGFP) filter cube BP490nm/535nm (Omega Optical) and the emitted light was collected at 530 nm (BP 530/20 nm, Omega Optical). Patch pipettes were pulled from a standard borosilicate glass (OD 1.5 mm, Sutter BF-150) on a horizontal micropipette puller (P-87, Sutter Instruments) and fire polished. Electrodes were filled with a normal Ringer containing (mM): 140 NaCl, 5 KCl, 1 $MgCl_2$, 1 $CaCl_2$, 10 HEPES (4-(2-hydroxyethyl)-1-piperazineethanesulfonic acid), and pH 7.4. Typical seal resistance in the loose-patch configuration was 40–80 Mohms. Recordings of spontaneous and odor-evoked extracellular action potentials were low-pass filtered ay 5 kHz and sampled at 10 kHz using an Axopatch 200A amplifier connected to analog-to-digital signal converter interface (Digidata 1320) controlled by Clampex 9.2 software (Molecular Devices). Recording was performed during the light phase of the light:dark cycle (between 0800 and 1700 hours). Offline analysis of electrophysiological recordings and action potential sorting were performed, without filtering, using Clampfit 10.7 and SigmaPlot 11 (SPSS) software.

ORNs that discharged with inherent bursts, referred to herein as bORNs, were identified as a cohort from canonical tonically active ORNs by the following criteria: 1) an inherent burst-like pattern of spontaneous discharge, 2) the virtual absence of nonburst discharge (single action potentials) between bursts, and 3) their response to odor stimulation with a burst of similar structure to their inherent burst structure. We did not systematically study the effect of odorant concentration on burst structure in this study, although it would be expected to have an effect. From casual observation in mammals and more formal analysis in lobsters, however, odor concentration does not change burst structure outside of the normal variation of the burst structure for any given cell. The interburst intervals (IBIs) and burst structure in bORNs were determined using the burst analysis protocol provided in pCLAMP. A burst delimiting interval (typically 100–500 ms) and a minimum number of spikes in a burst (typically 5) were individually specified for each ORN. IBIs were calculated as the time between the first spikes of 2 subsequent bursts. The time of occurrence of the spike was taken as the time of positive or negative peak current deflection.

Confocal en face calcium imaging of the semi-intact olfactory epithelium

For imaging, a small piece of the MOE dissected in oxygenated ACSF was mounted in a perfusion chamber (RC-26, Warner Instruments) with the apical surface facing down. The chamber was transferred to the stage of a Nikon TiE-PFS-A1R confocal microscope equipped with a 488-nm laser with a 510–560-nm band-pass filter and a ×60 oil-immersion (1.4 N.A) objective lens. Time-series acquisition was performed with 256 × 256 pixel resolution at the rate of 2 frames per second. The tissue was kept under continuous perfusion of freshly oxygenated ACSF throughout the experiment. Imaging was performed within the layer of cell bodies 30–50-µm deep in the tissue. Despite using a single photon imaging, the transparency of the tissue provided sufficient signal-to-noise ratio to resolve individual cell bodies. Each cell was assigned a region of interest (ROI), and changes in fluorescence intensity within each ROI were analyzed and expressed as the peak fractional change in fluorescent light intensity

ΔF/Fo, where Fo is the baseline fluorescence. Only cells with a peak amplitude of oscillation 2 standard deviations greater than the average basal fluorescent intensity level, as fit by eye, were identified as calcium transients associated with bursts and included in the analysis. As indicated in Figure 3A, significant calcium transients are only associated with neural bursts. Analysis and graphical presentation of the calcium imaging data were performed with pClamp 10.7 (Molecular Devices), NIH ImageJ software (https://imagej.nih.gov/ij), and Sigma Plot 11 (SPSS).

Odor stimulation

Mouse and rat ORNs were stimulated using a defined odorant applied by 10 psi pressure pulses for 100 msec duration from a glass micropipette positioned 100 µm away from the recorded ORN knob. The shading used in the figures to represent the stimulus application does not accurately reflect the stimulus intensity profile. To have maximal chance of finding a responsive cell, nontagged unidentified ORNs (in rat and mouse) were stimulated with a complex odor mix (Henkel-100; Wetzel et al. 1999) diluted 1:10^5 in ACSF, which is below the average EC_{50} of 1:$10^{4.55}$ (Ukhanov et al. 2010). Optically identified, GFP-expressing mouse M71 ORNs were stimulated with 1-µM acetophenone, which is below the average EC_{50} of 20µM (Bozza et al. 2002).

Results

Comparison of the response characteristics of a novel population of rhythmically active ORNs (bORNs) versus canonical tonically active ORNs in mice

Patch clamping the dendritic knobs of 73 ORNs in semi-intact MOE preparations obtained from 5 WT C57/BI6 mice showed that 60 (82.2%) of the ORNs were canonical tonically active cells (Figure 1A). The level of spontaneous activity of the tonically active cells varied. Some were characterized by relatively regular spiking (Figure 1A, top panels). Most, however, generated spikes in a less coherent manner (Figure 1A, middle and bottom panels). Figure 1C summarizes the overall distribution of spontaneous activity across this cohort. Despite the difference in spontaneous activity, all the cells in this cohort responded to odor stimulation with a transient increase in firing rate, as shown for one such ORN at one odor concentration in Figure 1B.

In contrast, the remainder of the ORNs (13, 17.8%) were rhythmically active and discharged in bursts of action potentials rather than generating stochastically distributed action potentials (Figure 2D). We refer to these ORNs herein as bORNs. bORNs were identified as a cohort using the criteria listed in Methods. bORNs had different burst frequencies and burst structure (Figure 1D). Some cells have relatively regular periodicity (Figure 1D, top panels), whereas others are less regular (Figure 1D, middle and bottom panels). Overall, the bursting frequencies of the bORNs from these and the other mice used in this study ranged from 0.08 to 0.77 Hz (F_b = 0.30 ± 0.31 Hz, n = 37; Figure 1F). The recording in Figure 1D (middle panels), which captured both a bORN (large spike) and a canonical tonically active cell (small spike), helps contrast the difference in the background discharge between the 2 subpopulations. Because the bORNs rhythmically discharge in the absence of odor stimulation, we refer to them as "inherent oscillators," as opposed to "conditional oscillators" that would only rhythmically discharge in response to prolonged odor stimulation or some other external perturbation. The bORNs respond to odor stimulation with an evoked burst similar in structure to the cell's spontaneous bursts (Figures 1E and 2D). They respond in a phase-dependent manner. That means whether they generate an odor-evoked burst is dependent on the time since the preceding spontaneous burst, that is, when the odor arrived relative to that particular cell's "entrainment window." If the odor arrives too soon after the last spontaneous burst, there is no evoked burst, whereas if the odor arrives within the cell's entrainment window, the next spontaneous burst is phase shifted (Figure 1E).

Figure 2 characterizes the response of bORNs in more detail. As shown for another bORN (Figure 2A), the probability of evoking a burst is a sigmoid function of the time since the last spontaneous burst and the time of arrival of the odor pulse ($Pe(\Phi)$; Figure 2B, dark plot). This contrasts to the probability density function (PDF) for the spontaneous bursts in the same cell (Figure 2B, gray bars and Gaussian). Expressing the PDF as cumulative probability function (CFP) (Figure 2C, $F(\Phi)$, gray bars and sigmoid) shows the probability of spontaneous burst occurrence within the time interval since the previous burst. Plotting the difference between the evoked burst cumulative probability function (CPF) (Figure 2B, C) and the spontaneous burst CPF (Figure 2C, gray histogram and line) gives the "tuning characteristic" for the cell (Figure 2C, bell-shaped curve) relative to stimulus time. That is, it specifies the frequency/phase range where a stimulus of a given intensity would be most efficient entraining the spontaneous burst rhythm. bORNs with different spontaneous bursting frequencies had different tuning curves (Figure 2E), allowing the population of bORNs to encode a range of stimulus intermittencies. Note that the spontaneous and evoked bursts have similar structure (Figure 2D) as was true of all cells tested (data not shown).

bORN-like activity imaged in the MOE from OMP-GCaMP6f mice

The ability of bORNs to respond to odors would argue they are mature, functional ORNs. To provide more direct evidence that bORNs are mature ORNs, that their rhythmic activity indeed reflects the output of the ORN, and to obtain a larger sample size, we imaged the soma layer of the MOE of OMP-GCaMP6f mice. Of 4928 cells imaged and analyzed for their activity, 4290 (87.1%) were canonical tonically active cells. In contrast, the remainder of the ORNs (638, 12.9%) were rhythmically active as evidenced by spontaneous calcium oscillations (Figure 3C, D). We assume these calcium oscillations reflect neural bursting of the cells. Indeed, simultaneous recording of the calcium oscillations and the neural discharge for 3 of the cells confirmed that the calcium oscillations correlate with neural burst discharges as shown for one cell in Figure 3A. As would be expected, the peak of the burst spike timing histogram falls within the rising phase of the calcium signal oscillations (Figure 3B). Overall, the frequency of the calcium oscillations of the rhythmically active ORNs ranged from 0.008 to 1.4 Hz (F_b = 0.16 ± 0.01 Hz, n = 161; Figure 3E).

Comparison of the incidence of bORNs versus canonical tonically active ORNs in mice with identified ORs

In order to get an initial understanding of the dependency of rhythmic activity on the endogeneous OR, we compared the relative number of bORNs obtained from 2 transgenic mouse lines in which ORNs expressing a known OR could be identified, M71/SR1-ires-tauGFP

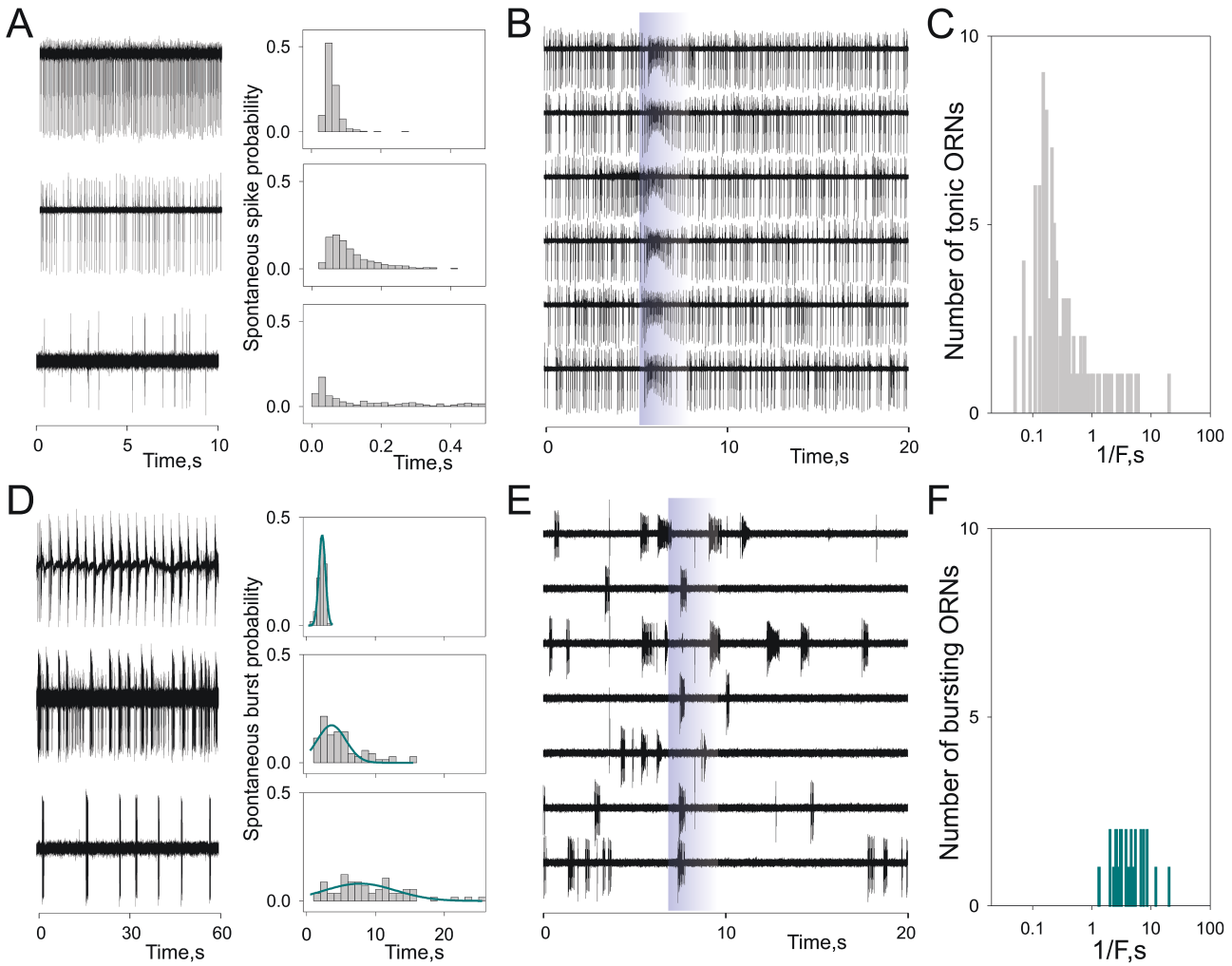

Figure 1. General characteristics of 2 subpopulations of ORNs recorded from WT mice. (**A–C**) Canonical tonically active ORNs. (A) Spontaneous activity of 3 different tonically active cells showing variability in the regularity of their spontaneous discharge. Some cells are characterized by relatively regular spiking (top panels), whereas most generate spikes in a less coherent manner (middle and bottom panels). Interspike interval (ISI) histograms were generated using at least 100-s intervals; bin width: 20 ms. Basal spiking frequencies of the ORNs shown range from 2 to 22.8 Hz. (B) Tonically active cells respond to an odor stimulus (shading) with a transient stimulus-dependent change in firing rate as shown for the same ORN as in A (middle panels), which responds transiently and consistently to a 500-msec odor pulse (6 responses shown). (C) Plot of the overall spontaneous frequency (1/*F*) distribution calculated for 100 tonically active ORNs. The spontaneous spike frequency of each cell was determined for at least 60 s. Histogram bin width: 20 ms. (**D–F**) bORNs. (D) In contrast to A, the cells spontaneously discharge in bursts (note the compressed time base compared with A). Some cells are characterized by relatively regular bursting (top panels), whereas others are less regular (middle and bottom panels). For the PDFs, the IBIs were estimated over at least 2 min of spontaneous activity. Gaussian fits to the PDFs are shown in the dark lines. Note that the middle trace shows a fortuitous simultaneous recording from 2 different ORNs, one a bORN (larger spike) and the other a canonical tonically active ORN (smaller spike). (E) In contrast to B, bORNs respond to odor stimulus (shading) by generating bursts, but the evoked burst probability is phase dependent, that is, it depends on the time since the preceding spontaneous burst. If the odor arrives early in the spontaneous bursting cycle, the evoked burst probability is low. (F) Plot of the overall spontaneous bursting frequency (1/F) distribution calculated for 37 bORNs. The spontaneous bursts frequency of each cell was determined for at least 60 s. Histogram bin width: 20 ms. See Methods for details of the electrophysiological recording. This figure is reproduced in color in the online version of this issue.

and I7>M71-ires-tauGFP mice. Patching the dendritic knobs of 67 M71-GFP ORNs from 17 transgenic mice revealed that 59 (88.1%) were canonical tonically active ORNs, whereas 8 (11.9%) were bORNs. Patching the dendritic knobs of 37 I7-GFP ORNs from 10 transgenic mice revealed that 36 (97.3%) were canonical tonically active ORNs, whereas 1 (2.7%) was a bORN. We also patched the dendritic knobs of 15 SR1-GFP ORNs in the septal organ from 3 transgenic mice. Of these 15 ORNs, 14 (93.3%) were canonical tonically active cells, whereas 1 (6.7%) was a bORN. These results show that both bORNs and canonical active ORNs can express the same receptor and argue that they potentially share the same odor specificity, although they do not eliminate possible bias in overall distribution of receptors between the 2 subpopulations that could emerge with a larger sample size. They also give no insight into potential difference in the breadth of tuning of bORNs versus that of canonical tonically active ORNs. Those potential distinctions await further experimentation.

Properties of bORNs in mice generalize to rats

We briefly addressed whether the findings in mice generalize to rats. As with mice, the majority (184, 80%) of ORNs sampled by patching the dendritic knobs of 230 ORNs from 8 rats were canonical tonically active cells that responded to odor application with a

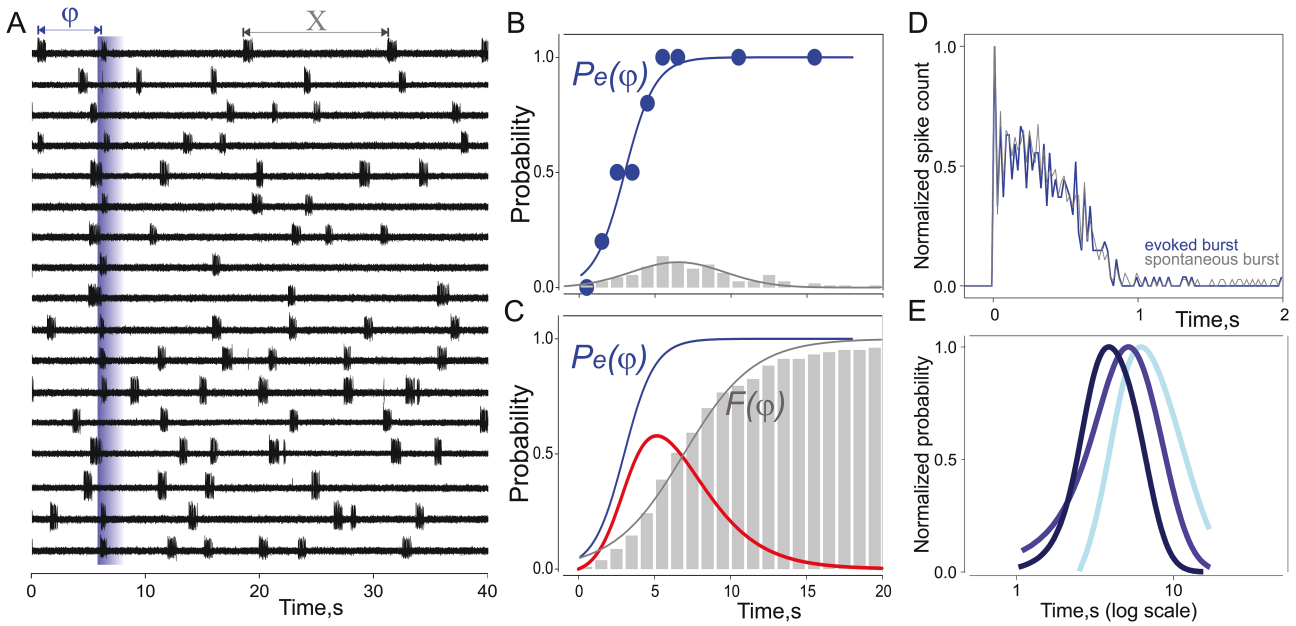

Figure 2. Further analysis of the odor-evoked activity in bORNs recorded from WT mice. (**A**) Extracellular single unit recording of spontaneous and evoked bursts from the same ORN. Stimuli were always applied independently of any ongoing activity, but the trials are aligned relative to the time of stimulus application. (**B**) Plot of the cumulative probability of eliciting a burst in the cell shown in A in response to an odorant (solid circles and sigmoid fit) as a function of the time since the last burst and odorant pulse (CPF, *Pe*(φ)). Probability estimated over 1-s intervals. Superimposed on the plot is the IBI histogram normalized to the total number of IBIs, which reflects the PDF for the spontaneous bursts (bars and Gaussian fit). Bin width: 1 s. (**C**) Plot of the "tuning" of the cell shown in A. The PDF is expressed here as a CPF (*F*(φ), bars and sigmoid fit), which reflects the probability of spontaneous burst occurrence within the time interval since the previous burst. The difference between the evoked CPF (reproduced here from B) and the spontaneous burst CPF gives the "tuning" of the cell relative to time (dark bell-shaped curve). The tuning function specifies the frequency/phase range where a stimulus of a given intensity would be more efficient entraining the spontaneous burst rhythm, for this cell about 5 s. (**E**) Different cells (3 shown) have different tuning functions. (**D**) Plot of the burst structure of the cell shown in A showing that the spontaneous and evoked bursts have similar structure. Bursts were aligned relative to the first spike. Histograms were generated using an 20-ms bin width and normalized relative to the number of bursts analyzed (n = 38 spontaneous, 27 evoked). See Methods for details of the electrophysiological recording. This figure is reproduced in color in the online version of this issue.

transient increase in discharge frequency (Figure 4A). As with mice, the spontaneous activity across the sample of canonical tonically active cells ranged primarily between 0.1 and 10 Hz (Figure 4B). As with mice, the remainder of the rat ORNs studied (46, 20%) were inherently rhythmically active, discharging in bursts of action potentials rather than single action potentials, and in which excitatory odor input entrained the intrinsic rhythm of bursting (Figure 4C). Overall, the range of inherent bursting frequencies in rats was broader than that in mice, ranging from 0.02 to 2.60 Hz, although the mean bursting frequency was similar to that in mice (F_b = 0.34 ± 0.07 Hz, n = 46) (Figure 4D).

Discussion

Here, we characterize the dynamic properties of a functional subset of mouse ORNs that can potentially encode olfactory information by having their rhythmicity entrained by the odor stimulus. Such internal representation of interval timing is typically associated with higher order brain function and can involve various central neural mechanisms (e.g., Miall 1989; Buhusi et al. 2005; Bueti 2011; Laje and Buonomano 2013). Although oscillatory network dynamics have been strongly implicated in deciphering the temporal structure of odor stimuli in locusts (Brown et al. 2005), peripheral mechanisms such as a system of peripheral uncoupled oscillators suggested by the present data represent a novel mechanism for encoding interval timing. Indeed, the bORNS do not respond to odorants by discharging phaso-tonically as do canonical tonic mammalian ORNs, so they represent a heretofore unappreciated way of encoding olfactory information. Our finding that 12.9% of the mature ORNs in the mouse MOE estimated by ensemble imaging and that 20% of the mature ORNs in the rat MOE estimated by physiological recording are rhythmically active argues that the input mediated by this subset of ORNs is functionally significant. The difference in incidence between the 2 species not only could reflect the difference in sample size but may also suggest that the incidence of bORNs is a species-dependent variable. Larger samples will be required to rigorously determine the actual incidence of bORNs.

As mentioned, oscillatory ORNs have been previously reported in amphibians (Reisert and Matthews 2001a) and mice (Sicard 1986; Reisert and Matthews 2001b). The most notable difference between the earlier findings and those reported herein is that the oscillations in the earlier studies were (or could have been; Sicard 1986) evoked in response to prolonged odor stimulation, that is, the oscillations were conditional, whereas those reported herein are inherent, that is, they exist in the absence of odor stimulation, although a small number of inherent oscillatory ORNs were reported in frog (Reisert and Matthews 2001a). Where measured, the oscillation periods fell in the same general range as those reported here: 3.5 to 12 s in frog and 0.4 to 2.4 s in mouse versus 1–10 s in the present study (Figure 1F). In both the earlier and the present studies, the oscillation periods were relatively constant for individual cells. Although the oscillation periods were constant at different odor concentrations for a given cell in frog (Reisert and Matthews 2001a), a 2–3-fold increase in odor concentration reduced the oscillation period in individual cells

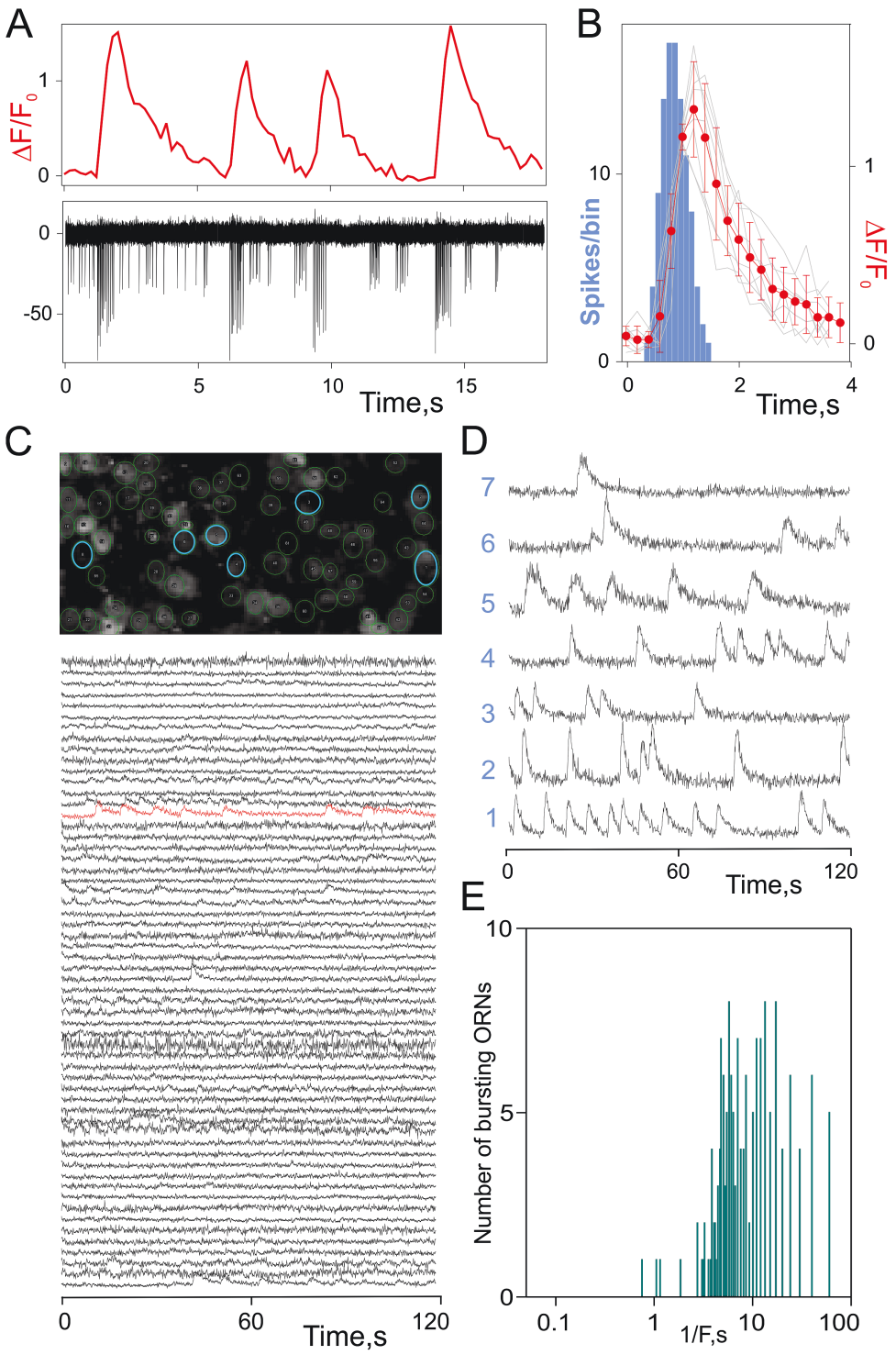

Figure 3. Spontaneous calcium oscillations in OMP-GCaMP6f mouse ORNs. (**A**) simultaneous measurement of the calcium signal (top) and the spike discharge (bottom) from an ORN exhibiting spontaneous calcium oscillations. (**B**) Plot showing the correlation between the peak of the burst-related spike timing histogram and the peak of the average calcium signal oscillation (solid circle and curve). Burst parameters: number of spikes per burst = 16; IBI = 9.1 s; burst duration = 0.7 s. Error bars are standard deviations. Bin width –0.1 s. (**C**) (bottom) Representative fluorescence intensity traces for a subset of 65 of the ORNs analyzed. Slow changes in the level of the calcium signal due to bleaching were manually subtracted. (C) (top) Fluorescent micrograph showing 7 areas of interest (open circles) delimiting 7 of 11 ORNs exhibiting spontaneous calcium oscillations. (**D**) Fluorescence intensity traces from the 7 ORNs indexed in the micrograph. (**E**) Plot of the overall spontaneous calcium oscillation frequency (1/F) distribution calculated for 161 ORNs.The spontaneous oscillation frequency of each cell was determined for at least 120 s. See Methods for details of the imaging and electrophysiological recording. This figure is reproduced in color in the online version of this issue.

between 10% and 50% in mouse (Reisert and Matthews 2001b). We did not test the effect of odor concentration in the present study, but increasing the stimulus strength increases the reliability of entrainment of bORNs in lobster (Bobkov and Ache 2007). That finding would not be inconsistent if what was being observed in the earlier study with mice was "tightening" of the oscillation period

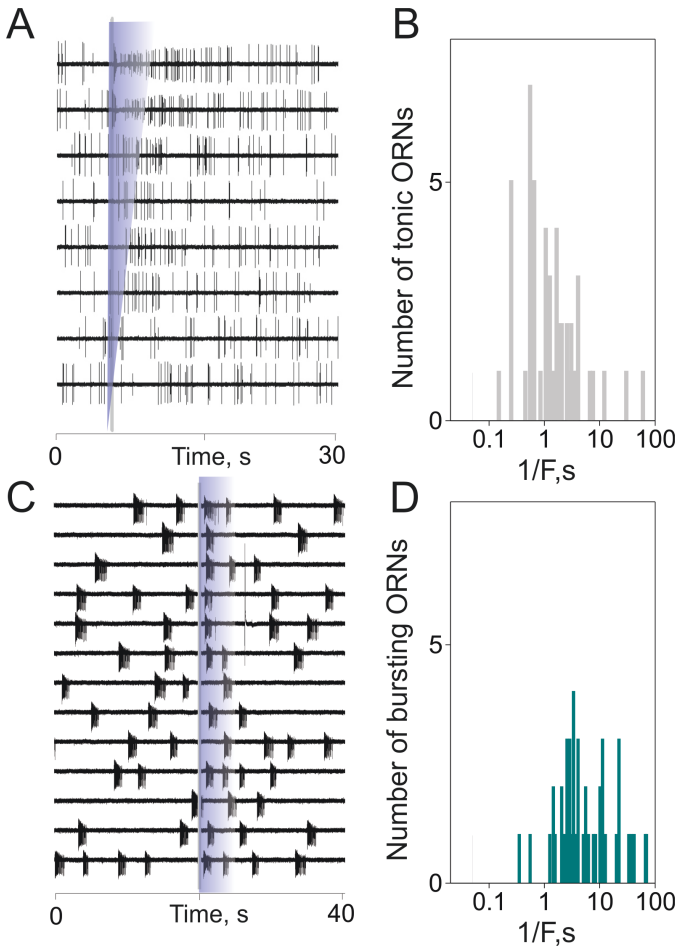

Figure 4. Electrophysiological recording from a canonical tonically active ORN (**A, B**) and a bORN (**C, D**) in rats. (A) Spontaneous and odor-evoked activity of a tonically active ORN. The ORN responds phasically to subsequent odor stimulation at increasing stimulus intensity (shading, lowest intensity at the bottom). (B) Plot of the spontaneous spike frequency (1/*F*) distribution of the tonically active ORNs surveyed ($n = 184$, bin width = 100 ms). (C) Spontaneous and odor-evoked activity of a bORN. The odor (shading) was applied at random and 20 s of activity on either side of the odor stimulation was captured and aligned to the period of stimulation. Note that the odor resets the phase of (entrains) the bORN only when the arrival of the odor falls within a certain interval following the last spontaneous burst (the entrainment window) of the ORN. Stimulus parameters in this case were identical for all traces. (D) Plot of the spontaneous bursting frequency (1/*F*) distribution of the bORNs ($n = 46$). Bursting parameters of individual ORNs were estimated over 60–200 s intervals. Bin width: 100 ms. See Methods for details of the electrophysiological recording. This figure is reproduced in color in the online version of this issue.

with increasing stimulus strength. However, the earlier study did not investigate possible odor-dependent entrainment of the rhythmicity. Further research needs to be directed toward understanding these differences, as well as reports of potential burst coding in mouse vomeronasal sensory neurons (Arnson and Holy 2011).

Our using the term "inherent oscillators" to differentiate the cells in the present study from "conditional oscillators" is not meant to imply that the origin of the rhythmicity is physiologically inherent in mammalian bORNs. Because all the neurons reported were recorded or imaged in the semi-intact MOE, we cannot exclude that their rhythmicity was imposed or modulated by synaptic and/or ephaptic interactions with other cells in the MOE. However, our ability to record canonical and rhythmic activity in the same patch of semi-intact MOE argues that, if direct or indirect connectivity imposes rhythmicity, it must not generalize across the MOE, and there is no evidence that mammalian ORNs and supporting cells (SUSs) are grouped in stereotyped functional combinations that would be required to explain that alternative. In addition, the ability to record rhythmicity in acutely dissociated mammalian bORNs argues that rhythmicity can be inherent in these cells (Ukhanov, unpublished data).

Although we lack sufficient numbers to computationally model mammalian bORNs, given that their ensemble dynamic properties align with those described earlier for lobster bORNs (Park et al. 2014) allows us to speculate on the potential functional significance of mammalian bORNs. That is, we would predict that, as a population, mammalian bORNs can accurately encode the interval since the last odor encounter and do so instantaneously without the need to implicate memory. That, of course, remains to be tested. The difference in the mean bursting frequency of bORNs in mice ($F_b = 0.30 \pm 0.03$ Hz, $n = 31$) and rats ($F_b = 0.35 \pm 0.07$ Hz, $n = 46$) did not differ appreciably from that of bORNs in lobsters ($F_b = 0.22 \pm 0.02$ Hz, $n = 92$; Bobkov and Ache 2007), although any difference could potentially reflect adaptation to the dynamic properties of the odor worlds in which the 2 animals live. We would further speculate based on the ensemble properties of lobster bORNs that odor time serves as a more efficient means to navigate odor plumes than does odor concentration (Park

et al. 2016). The potential for blocking mammalian bORN input by pharmacologically targeting the different types of ion channels known to underlie neural oscillations and studying the behavior of genetically modified mice in which the appropriate in channel(s) are conditionally deleted should allow experimental verification of this latter speculation.

In understanding the potential functional significance of mammalian bORNs, it is important to appreciate that the range of intermittencies encoded by bORNs is dynamically unrelated to sniffing intermittency. As a population, bORNs have the potential to encode the intermittency inherent in turbulent odor environments, which can range from hundreds of msecs to tens of secs (e.g., Vickers et al. 2001; Celani et al. 2014; Riffell et al. 2014). In contrast, sniffing is fast, 2–12 Hz in mice (e.g., Wesson et al. 2008), and consequently would confound encoding only the shortest intermittency inherent in the odor environment. Even if extremely brief intermittency could be behaviorally salient, that would be a trade-off the animal might make given the gain in odor detection conferred by sampling intermittency (e.g., Schmitt and Ache 1979).

We have yet to understand the target of bORN input in the mammalian central nervous system (CNS). Our finding that mouse ORNs expressing the same OR can be either bORNs or canonical tonically active ORNs would suggest both subsets target common glomeruli because it's generally assumed that all ORNs expressing the same OR target a pair of common ipsilateral glomeruli (e.g., Mombaerts et al. 1996). This finding does not necessarily mean that specification of rhythmic activity is independent of the OR, however. We show a possible OR-specific difference in the ratio of bORNS to canonical tonically active ORNS, allowing the OR may play a role in determining that ratio across the population. Such complexity would be consistent with earlier findings that the role of the OR in controlling cell function is more complex than originally suspected (e.g., Reisert 2010; Connelly et al. 2013). How the 2 inputs would be subsequently processed at the first olfactory relay remains to be determined. Recent evidence that a subset of mitral-tufted cells in the MOB of mice encode turbulent fluctuations in odor concentration implies that the spatial-temporal aspects of the odor signal and, therefore, potentially bORN input could be processed in parallel with odor identify information within the MOB (Lewis et al. 2018).

Given the evidence that bORN-based encoding of olfactory information described in lobsters extends to rodents, it is interesting to speculate that bORN-based coding is a fundamental feature of olfactory organization. If so, our current understanding would suggest that bORN-based encoding of olfactory information may have evolved in animals to facilitate navigating turbulent odor plumes in air and water, perhaps odor plumes within a certain range of dynamic characteristics.

Acknowledgement

We thank Dr Minghong Ma (Department of Neuroscience, University of Pennsylvania) for the M71/SR1-ires-tauGFP and the I7>M71-ires-tauGFP mice.

Funding

The research reported here was supported by the National Institute on Deafness and Other Communication Disorders (DC011859 to B.W.A; DC009606 to J.R.M.) and by the National Science Foundation through a cooperative award to B.W.A. (Project 1631787), Dr Jose Principe (Department of Electrical and Computer Engineering, University of Florida; Project 1631759), and Dr Matthew Reidenbach (Department of Environmental Engineering, University of Virginia; Project 1631864).

Conflict of Interest

The authors declare no conflicts of interest

References

Arnson HA, Holy TE. 2011. Chemosensory burst coding by mouse vomeronasal sensory neurons. *J Neurophysiol*. 106:409–420.

Bobkov YV, Ache BW. 2007. Intrinsically bursting olfactory receptor neurons. *J Neurophysiol*. 97:1052–1057.

Bozza T, Feinstein P, Zheng C, Mombaerts P. 2002. Odorant receptor expression defines functional units in the mouse olfactory system. *J Neurosci*. 22:3033–3043.

Brown SL, Joseph J, Stopfer M. 2005. Encoding a temporally structured stimulus with a temporally structured neural representation. *Nat Neurosci*. 8:1568–1576.

Buhusi CV, Perera D, Meck WH. 2005. Memory for timing visual and auditory signals in albino and pigmented rats. *J Exp Psychol Anim Behav Process*. 31:18–30.

Bueti D. 2011. The sensory representation of time. *Front Integr Neurosci*. 5:34.

Celani A, Villermaux E, Vergassola M. 2014. Odor landscapes in turbulent environments. *Phys Rev*. 4:041015.

Connelly T, Savigner A, Ma M. 2013. Spontaneous and sensory-evoked activity in mouse olfactory sensory neurons with defined odorant receptors. *J Neurophysiol*. 110:55–62.

Grosmaitre X, Fuss SH, Lee AC, Adipietro KA, Matsunami H, Mombaerts P, Ma M. 2009. SR1, a mouse odorant receptor with an unusually broad response profile. *J Neurosci*. 29:14545–14552.

Laje R, Buonomano DV. 2013. Robust timing and motor patterns by taming chaos in recurrent neural networks. *Nat Neurosci*. 16:925–933.

Lewis SM, Park J, Tariq MF, Seminara A, Gire DH. 2018. Sensory encoding of natural odor dynamics by mitral and tufted cells in the olfactory bulb. *Soc Neurosci Abstr*. 217:06/Y16.

Madisen L, Garner AR, Shimaoka D, Chuong AS, Klapoetke NC, Li L, van der Bourg A, Niino Y, Egolf L, Monetti C, et al. 2015. Transgenic mice for intersectional targeting of neural sensors and effectors with high specificity and performance. *Neuron*. 85:942–958.

Miall C. 1989. The storage of time intervals using oscillating neurons. *Neural Comp*. 1:359–371.

Mombaerts P, Wang F, Dulac C, Chao SK, Nemes A, Mendelsohn M, Edmondson J, Axel R. 1996. Visualizing an olfactory sensory map. *Cell*. 87:675–686.

Park IM, Bobkov YV, Ache BW, Príncipe JC. 2014. Intermittency coding in the primary olfactory system: a neural substrate for olfactory scene analysis. *J Neurosci*. 34:941–952.

Park IJ, Hein AM, Bobkov YV, Reidenbach MA, Ache BW, Principe JC. 2016. Neurally encoding time for olfactory navigation. *PLoS Comp Biol*. 12(1):e1004682.

Reisert J. 2010. Origin of basal activity in mammalian olfactory receptor neurons. *J Gen Physiol*. 136:529–540.

Reisert J, Matthews HR. 2001a. Responses to prolonged odour stimulation in frog olfactory receptor cells. *J Physiol*. 534:179–191.

Reisert J, Matthews HR. 2001b. Response properties of isolated mouse olfactory receptor cells. *J Physiol*. 530:113–122.

Riffell JA, Shlizerman E, Sanders E, Abrell L, Medina B, Hinterwirth AJ, Kutz JN. 2014. Flower discrimination by pollinators in a dynamic chemical environment. *Science*. 344:1515–1518.

Schmitt BC, Ache BW. 1979. Olfaction: responses of a decapod crustacean are enhanced by flicking. *Science*. 205:204–206.

Shraiman BI, Siggia ED. 2000. Scalar turbulence. *Nature*. 405:639–646.

Sicard G. 1986. Electrophysiological recordings from olfactory receptor cells in adult mice. *Brain Res*. 397:405–408.

Ukhanov K, Corey EA, Brunert D, Klasen K, Ache BW. 2010. Inhibitory odorant signaling in Mammalian olfactory receptor neurons. *J Neurophysiol*. 103(2):1114–1122.

Vergassola M, Villermaux E, Shraiman BI. 2007. "Infotaxis" as a strategy for searching without gradients. *Nature*. 445:406–409.

Vickers NJ, Christensen TA, Baker TC, Hildebrand JG. 2001. Odour-plume dynamics influence the brain's olfactory code. *Nature*. 410:466–470.

Wesson DW, Donahou TN, Johnson MO, Wachowiak M. 2008. Sniffing behavior of mice during performance in odor-guided tasks. *Chem Senses*. 33:581–596.

Wetzel CH, Oles M, Wellerdieck C, Kuczkowiak M, Gisselmann G, Hatt H. 1999. Specificity and sensitivity of a human olfactory receptor functionally expressed in human embryonic kidney 293 cells and *Xenopus Laevis* oocytes. *J Neurosci*. 19:7426–7433.